Experimental and theoretical electronic structure of EuRh_{2}As_{2}

A. D. Palczewski, R. S. Dhaka, Y. Lee, Yogesh Singh, D. C. Johnston, B. N. Harmon, and Adam Kaminski

Phys. Rev. B **85**, 174509 — Published 11 May 2012

DOI: 10.1103/PhysRevB.85.174509

Experimental and theoretical electronic structure of $EuRh_2As_2$

A. D. Palczewski, R. S. Dhaka, Y. Lee, Yogesh Singh,* D. C. Johnston, B. N. Harmon, and Adam Kaminski†
Division of Materials Science and Engineering, The Ames Laboratory, US DOE,
and Department of Physics and Astronomy, Iowa State University, Ames, Iowa 50011, USA
(Dated: April 27, 2012)

The Fermi surfaces (FS's) and band dispersions of $EuRh_2As_2$ have been investigated using angle-resolved photoemission spectroscopy. The results in the high-temperature paramagnetic state are in good agreement with the full potential linearized augmented plane wave calculations, especially in the context of the shape of the two-dimensional FS's and band dispersion around the Γ (0,0) and X (π, π) points. Interesting changes in band folding are predicted by the theoretical calculations below the magnetic transition temperature $T_N \approx 47$ K. However, by comparing the FS's measured at 60 K and 40 K, we did not observe any signature of this transition at the Fermi energy indicating a very weak coupling of the electrons to the ordered magnetic moments or strong fluctuations. Furthermore, the FS does not change across the temperature (≈ 25 K) where changes are observed in the Hall coefficient. Notably, the Fermi surface deviates drastically from the usual FS of the superconducting iron-based AFe_2As_2 parent compounds, including the absence of nesting between the Γ and X FS pockets.

PACS numbers: 79.60.-i, 71.20.-b, 74.25.Jb

I. INTRODUCTION

The recent discoveries of superconductivity in FeAs-based materials, RLaFeAs($O_{1-x}F_x$) where R is a lanthanide element[1–5] and ($Ba_{1-x}K_x$)Fe_2As_2,[6,7] resulted in a large number of experimental and theoretical studies. These materials have revealed fascinating properties regarding the complex interplay among structure, magnetism and superconductivity,[8] especially the AFe_2As_2 (A = Ba, Sr, Ca, Eu) family of compounds with $T_{c,max} \approx 38$ K.[9–15] It has been shown that the parent compounds manifest simultaneous transitions where the high-temperature tetragonal paramagnetic phase changes at $\approx 140 - 205$ K to the lower-temperature orthorhombic phase with antiferromagnetic order which is associated with a spin density wave (SDW) and superconductivity is achieved in different ways.[6,9,10,16–19] There has been a flurry of activity trying to understand the basic properties of these new materials, and in particular, the mechanism for high T_c where the Fermi surfaces (FS's) play an important role.[20–22]

The key feature common to these materials is the presence of stacked FeAs layers. This gives a strong motivation to investigate similarly structured compounds in a search for additional high T_c superconductors and to understand the mechanism of the superconductivity and magnetic ordering. More recently, several isostructural materials have been found which show very interesting physical properties and can be potential parent compounds for high T_c superconductors, for example, $BaMn_2As_2$,[23], $EuRu_2As_2$,[24] $EuRh_2As_2$,[25,26] $BaRh_2As_2$,[27] and $SrRu_2As_2$.[28] The electronic structure of $BaNi_2As_2$, in particular, shows no signature of band folding suggesting the absence of SDW magnetic ordering.[29] Because these materials are not superconducting, the absence of Fe in these materials allows us to determine what role the Fe atoms play in superconductivity. Particularly, $EuRh_2As_2$ shows unusual characteristics that are not observed in the superconducting materials, including giant magnetoresistance and a strong reduction in the electronic specific heat coefficient with applied field in the antiferromagnetic state.[26] Magnetic scattering measurements reveal that the Eu spins are ferromagnetically aligned within the a-b plane where the spins between adjacent Eu planes are nearly antiparallel.[25] A previous calculation suggested that the maximum contribution in the electronic density of states at the Fermi energy (E_F) is from the Rh 4d orbitals.[26] Considering that the electronic states near the FS are dominated by contributions from the transition metal element, understanding the interplay between Rh and As at the FS is vital for these materials. To the best of our knowledge, there are no previous reports on the Fermi surfaces of $EuRh_2As_2$.

Here, we present the first angle-resolved photoemission spectroscopy (ARPES) study on $EuRh_2As_2$ detailing the three dimensional nature of the FS and comparing it to the theoretical full potential-linearized augmented plane-wave (FP-LAPW) calculations. We find that the FP-LAPW calculations predict the shape of the FS and general band dispersion quite well especially when comparing the data in the paramagnetic phase. Magnetic susceptibility and heat capacity measurements have demonstrated that $EuRh_2As_2$ undergoes a transition from a paramagnetic state to an antiferromagnetic state below the Néel temperature $T_N \approx 47$ K.[26] The ARPES data in the proximity of E_F do not show any signatures of this transition. Interestingly, the FS and band structure of $EuRh_2As_2$ are very different from those of other similar compounds including $EuFe_2As_2$[30,31] where the superconducting family has a hole band centered at Γ and electron band centered at X which are closely nested.[20,32] On the other hand, $EuRh_2As_2$ has electron bands centered at Γ and X with no evidence of nesting.

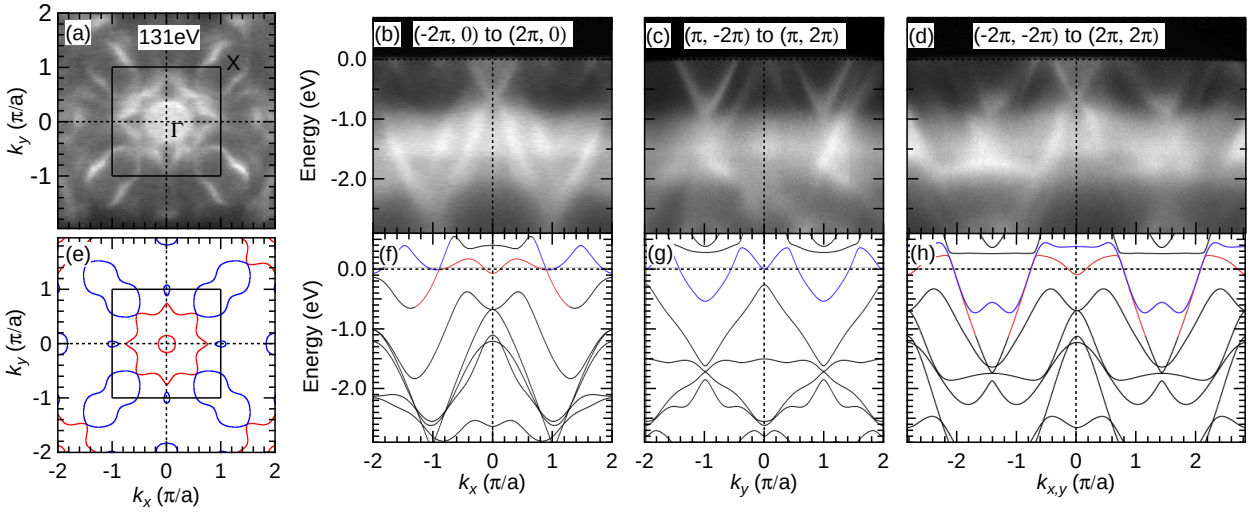

FIG. 1. (Color online) Comparison between the measured ARPES data (40 K) and the theoretical FP-LAPW calculations in the paramagnetic (high temperature) state: (a) measured FS of $EuRh_2As_2$ plotted within 50 meV of E_F over the first two Brillouin zones (BZ's) at 131 eV; (b–d) band dispersions from (a); (e–h) the same as (a–d) but calculated, colored lines denote predominant contributions from the Rh 4*d* (red) and the As 4*p* (blue) bands which cross E_F. The dashed squares in (a) and (e) bounded by −1 to 1 in k_x and k_y mark the first BZ boundary of the paramagnetic state (body-centered tetragonal structure). The directions of the band cuts are shown in each panel. The FP-LAPW FS calculation at $k_z = 3.5\ \pi/c$ ($h\nu = 131$ eV) in (e) shows the resulting calculated Fermi surface sheets using the same color coding.

II. EXPERIMENT

Single crystals of $EuRh_2As_2$ were grown out of Pb flux. X-ray diffraction measurements confirmed that $EuRh_2As_2$ crystallizes in the tetragonal $ThCr_2Si_2$ structure with lattice parameters $a = 4.075(4)$ Å and $c = 11.295(2)$ Å at 298 K.[26] Single crystal samples were cleaved *in–situ* at the base pressure of $\approx 4\times10^{-11}$ mbar. ARPES measurements were performed by using a Scienta R4000 electron analyzer on beamlines 7.0.1 and 10.0.1 at the Advanced Light Source (ALS), Berkeley, California. The energy and momentum resolution were set to $\sim$ 20 meV and $\sim 0.3°$, respectively. The polarization vector was parallel to the plane on incidence and the k_y direction for all data shown.

The FP-LAPW method with the local density approximation[34] was used to calculate the theoretical FS and band dispersions. To obtain self-consistent charge density, we employed $R_{MT} \times k_{max} = 8.0$ (the smallest muffin tin radius multiplied by the maximum k value in the plane wave expansion basis) with muffin tin (MT) radii of 2.5, 2.2, and 2.2 a_0 (Bohr radius) for Eu, Rh, and As, respectively. The calculations were carried out at 475 k-points in the irreducible Brillouin zone and the calculations were iterated to reach a total energy convergence criterion of 0.01 mRy/cell. While in the paramagnetic calculations the 4*f* electrons were treated as core electrons, a local-density-approximation plus Coulomb potential (LDA+U) method with $U = 5$ eV was used for the 4*f* electrons in the antiferromagnetic calculations.

III. RESULTS AND DISCUSSION

The FS was measured using two different photon energies of 131 eV (Figs. 1 and 3) and 105 eV (Fig. 2). They were chosen using a map along the $k_{||}$–k_z plane centered at $k_{x,y}(\pi/a)$ (*i.e.* k_z dispersion map obtained by scanning the photon energy – not shown). Note that, in the photoemission process, the component of the momentum of the outgoing electron perpendicular to the surface, *i.e.* k_z, is not conserved and creates an offset with respect to the high symmetry points. This non-conservation is due to the surface potential inherent in all materials, which can be calculated by measuring a k_z dispersion map and using $k_z = (1/\hbar)\sqrt{2m(E_k\cos^2\theta + V_0)}$, where E_k is the photoelectron kinetic energy and V_0 is the inner potential. In the map, we observe a non-integer k_z value at the symmetry points as compared to the calculations. Therefore, we included an energy shift (inner-potential) into the k value calculations which aligns the symmetry points to an integer k_z value at the symmetry point.[35,36] In the present case, the offset or inner-potential is estimated to be 8.9 eV, so that the k_z values for the two photon energies correspond to calculated ones with best agreement of the calculated and measured band dispersion.The two-dimensional FS plots of $EuRh_2As_2$ are shown in Figs. 1(a) and 2(a) measured using photon energies $h\nu$ =131 eV ($k_z = 3.5\ \pi/c$) and 105 eV ($k_z = 1.15\ \pi/c$), respectively, which correspond to two different symmetry points. It is quite remarkable that the FS [Figs. 1(a) and 2(a)] of $EuRh_2As_2$ are very differ-

ent from those of AFe$_2$As$_2$ (where A = Ba, Sr or Ca[37] as well as Eu[30,31]), where both electron and hole pockets are nearly nested.

Comparison of the measured ARPES data with theoretical calculations is vital for understanding the electronic structure of these materials. For this purpose, we have shown the experimental FS map at 131 eV ($k_z = 3.5\ \pi/c$) in the paramagnetic phase at 40K and the corresponding FP-LAPW calculations around the Γ $(0,0)$ point in Figs. 1(a) and 1(e), respectively. Both the measured as well as calculated FS's show two pockets centered at the Γ point and another pocket centered at X (π,π). This agreement shows that the FP-LAPW calculations reproduce our ARPES data quite well. Although the general shape of the pockets match, the size of these pockets do not, where the pocket at Γ is larger for the measured one. Unlike the FS at 105 eV (Figs. 2(a) and 2(e)), the FS pockets at the X point in Figs. 1(a) and 1(e) are quite similar without a significant matrix element effect. To examine the character of the FS pockets at the Γ and X points as measured using ARPES, which can usually be easily determined by tracing the dispersions of the associated bands, we compared the band dispersions along the symmetry points. The measured band dispersions are shown in Figs. 1(b–d) and the calculated band cuts are shown in Figs. 1(f–h). The symmetry cut lines are mentioned in the respective plots in Figs. 1 and 2. It is clear that the bands observed at the Γ and X points show an electron-like nature. All the measured band dispersions in Figs. 1(b–d) are in agreement with the respective calculations in Figs. 1(f–h) in terms of the shape. However, there are some differences in the size of the FS pockets. This is most likely due high sensitivity of the energy position of individual bands to relative ionic positions used in the calculation. It is likely that values somewhere in between the relaxed and experimentally measured ones would better fit the data.

To understand the three-dimensional nature of EuRh$_2$As$_2$ in detail, another photon energy hν = 105 eV ($k_z = 1.15\ \pi/c$) was chosen where the FS was measured and calculated [Figs. 2(a) and 2(e), respectively] along the a-b plane, which also show two pockets centered at Γ and another pocket centered at the X points (Fig. 2). The clearly visible crossing of the pocket centered at X in the second Brillouin Zone (BZ) matches roughly the shape of the calculated data, yet it is mostly not visible in the first BZ. This absence due to ARPES matrix element effect where certain transition probabilities are smaller and threfore observed.[38] By comparing the measured band dispersions in Figs. 2(b–d) with the calculated ones in Figs. 2(f–h), the nature of these pockets is clearly electron-like. Overall, the match between the data and calculations is not as good as for the previous case. For example we observe significant intensity at Ef close to $(-1.5\pi/a, 0.5\pi/a)$, even though no FS crossing is reported there in calculations. The exact energy locations of individual bands in the calculations strongly depends on the relative positions of ions, and is often difficult to reproduce over whole 3D BZ. It is possible that small adjustments somewhere between relaxed and experimental ionic positions would result in a better match. Note that the FS of the AFe$_2$As$_2$-type superconducting pnictides consist of closely nested pockets at Γ and X,[20,39–43] where the contributions from the Fe 3d orbitals dominate. This is not the case for EuRh$_2$As$_2$ where the FS pockets are electron-like with the contributions mainly from both Rh 4d electron bands at the Γ point and As 4p electron bands at the X point.

Previous transport studies on EuRh$_2$As$_2$[26] revealed two transition or crossover temperatures. These are the Néel temperature $T_N \approx 47$ K and the temperature where the Hall coefficient changes sign at $T \sim 25$ K. Above T_N, EuRh$_2$As$_2$ is in the paramagnetic body-centered-tetragonal state. Below T_N, the Eu moments are ferromagnetically aligned within the tetragonal a-b plane and nearly antiferromagnetic along the c axis.[25] The theoretical FP-LAPW calculations show a change in the FS upon crossing T_N, shown in Figs. 3(a) and 3(b) in the paramagnetic and antiferromagnetic phase, respectively. The calculations show a reduction of the BZ below T_N because the magnetic phase transition breaks the body-centered symmetry and doubles the unit cell. However, the ARPES data [Fig. 3(c) at 60 K and 3(d) at 40 K] do not show any signature of this back-folding. This might arise if the electrons do not couple to the ordered magnetic moments of the Eu ions or presence of significant fluctuations.[31,33] The Eu is divalent with seven 4f electrons. The Eu 5d bands begin about 1eV above the Fermi level, resulting in weak RKKY coupling and low ordering temperature. Another possibility is that the AF propagation vector in the k_z direction could cause the bands to overlap and hence no change would be present in the FS measured in the a-b plane. A previous study on EuRh$_2$As$_2$ showed no significant change in resistivity across T_N, while sharp transitions were observed at T_N in heat capacity and susceptibility measurements.[27] For EuFe$_2$As$_2$, it was shown that the Eu magnetic ordering does not have significant influence on the pre-existing Fe SDW ordering.[31]

Another transition or crossover occurs in EuRh$_2$As$_2$ where the Hall coefficient changes sign from negative to positive at around 25 K,[26] which is well below the magnetic transition temperature. This sign change was suggested to be a possible signature of temperature induced carrier redistribution between electron and hole like Fermi surfaces. In order to ascertain how the sign change in Hall coefficient would effect the FS, we measured the FS above and below this temperature (Fig. 4) *i.e.* at 44 K and 12 K, respectively. In Figs. 4(a) and 4(b), we present the FS measured at 37 eV, while Figs. 4(c) and 4(d) show the FS measured at 51 eV. Surprisingly, the data show no change in the FS between 44 K and 12 K. It possible that the changes in the FS related to the Hall effect do occur for other values of k_z than those explored in this work.

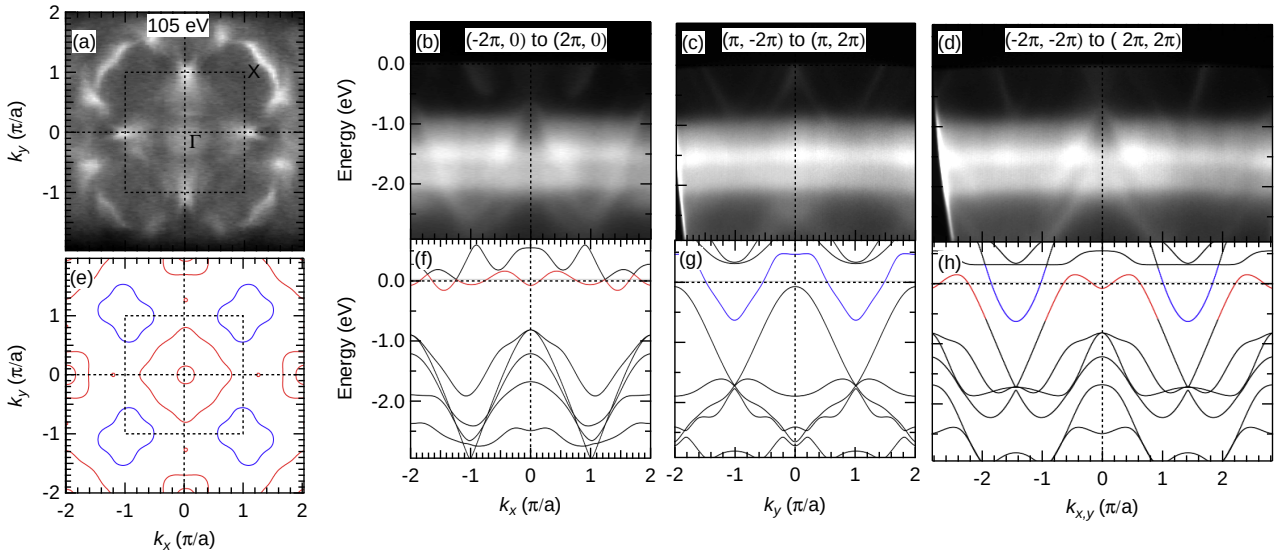

FIG. 2. (Color online) The FS and band dispersion plots, as defined in the caption of Fig. 1, except measured and calculated at $k_z = 1.15\ \pi/c$ (h$\nu = 105$ eV).

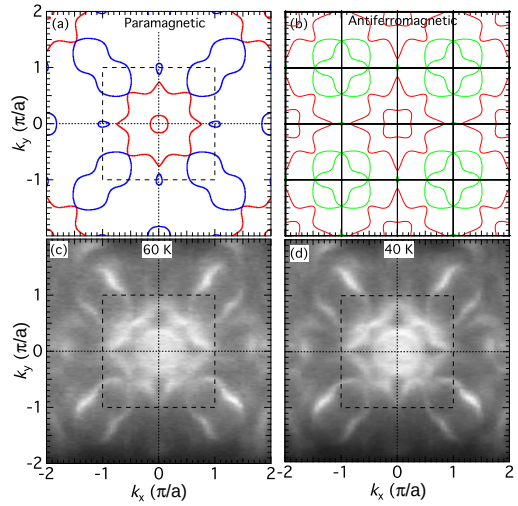

FIG. 3. (Color online) Comparison of the FP-LAPW calculations and the FS measured at $k_z = 3.5\ \pi/c$ (hν =131 eV) by ARPES above and below $T_N \approx 47$ K. Theoretically calculated FS at (a) high temperature paramagnetic and (b) low temperature antiferromagnetic states showing band back-folding caused by a doubling of the unit cell when the sample goes from a nonmagnetic body-centered tetragonal to a magnetic tetragonal structure. Colors in panel b are used for clarity and do not reflect particular orbital contributions. The measured FS at (c) 60 K paramagnetic and (d) 40 K antiferromagnetic states showing no change in the band structure.

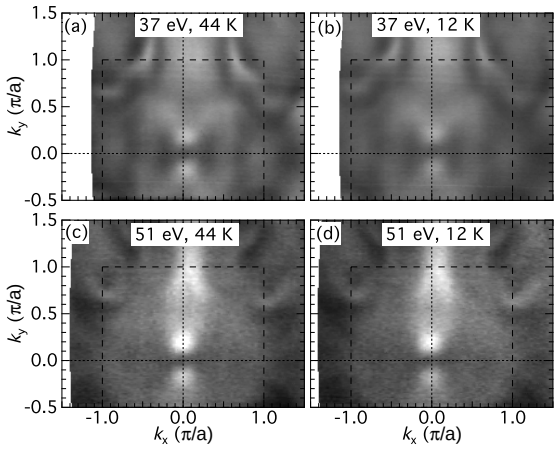

FIG. 4. The FS of $EuRh_2As_2$ above (44K) and below (12K) the temperature where the Hall coefficient changes sign ($\sim$ 25 K), plotted within $\pm$ 20 meV of E_F. The photon energy and measured sample temperature are shown in each panel.

IV. CONCLUSIONS

In conclusion, the Fermi surface of $EuRh_2As_2$ has been studied using ARPES and compared with the theoretical FP-LAPW calculations. The FP-LAPW calculations map the general shape of the FS and band dispersion quite well especially when compared to the high temperature paramagnetic data. We observed the signature of the three-dimensional nature of the FS. Surprisingly, the FS data do not show any indication of the AF state below the T_N implying a weak coupling between the Eu and RhAs layers at least in the studied parts of the BZ. Moreover, the sign change in the Hall coefficient below 25 K does not seem to correspond to visible changes in the FS at k_z locations reported here. Notably, the band structure of $EuRh_2As_2$ is very different than $A Fe_2As_2$

compounds including $EuFe_2As_2$[30,31] where the superconducting family has nested hole and electron bands centered at Γ and X, respectively,[39] whereas $EuRh_2As_2$ has electron bands centered at Γ and X without nesting.

We thank Eli Rotenberg and Sung-Kwan Mo for excellent support at the ALS. The work at the Ames Laboratory was supported by the Department of Energy-Basic Energy Sciences under Contract No. DE-AC02-07CH11358. The ALS is supported by the U.S. DOE under Contract No. DE-AC02-05CH11231.

---

* Present address: Indian Institute of Science Education and Research Mohali, Chandigarh 140306, India.
† kaminski@ameslab.gov

[1] Y. Kamihara, T. Watanabe, M. Hirano, and H. Hosono, J. Am. Chem. Soc. **130**, 3296 (2008).
[2] X. H. Chen, T. Wu, G. Wu, R. H. Liu, H. Chen, and D. F. Fang, Nature **453**, 761 (2008).
[3] T. Y. Chen, Z. Tesanovic, R. H. Liu, X. H. Chen, and C. L. Chien, Nature **453**, 1224 (2008).
[4] G. F. Chen, Z. Li, D. Wu, G. Li, W. Z. Hu, J. Dong, P. Zheng, J. L. Luo, and N. L. Wang, Phys. Rev. Lett. **100**, 247002 (2008).
[5] H. Takahashi, K. Igawa, K. Arii, Y. Kamihara, M. Hirano, and H. Hosono, Nature **453**, 376 (2008).
[6] M. Rotter, M. Tegel, and D. Johrendt, Phys. Rev. Lett. **101**, 107006 (2008).
[7] H. Q. Yuan, J. Singleton, F. F. Balakirev, S. A. Baily, G. F. Chen, J. L. Luo and N. L. Wang, Nature **457**, 565 (2009).
[8] C. De la Cruz, Q. Huang, J. W. Lynn, L. Jiying, W. Ratcliff II, J. L. Zaretski, H. A. Mook, G. F. Chen, J. L. Luo, N. L. Wang, and P. Dai, Nature **453**, 899 (2008).
[9] A. S. Sefat, R. Jin, M. A. McGuire, B. C. Sales, D. J. Singh, and D. Mandrus, Phys. Rev. Lett. **101**, 117004 (2008).
[10] N. Ni, S. L. Bud'ko, A. Kreyssig, S. Nandi, G. E. Rustan, A. I. Goldman, S. Gupta, J. D. Corbett, A. Kracher, and P. C. Canfield, Phys. Rev. B **78**, 014507 (2008).
[11] K. Sasmal, B. Lv, B. Lorenz, A. M. Guloy, F. Chen, Yu-Yi Xue, and C.-Wu Chu, Phys. Rev. Lett. **101**, 107007 (2008).
[12] A. Kreyssig, M. A. Green, Y. Lee, G. D. Samolyuk, P. Zajdel, J. W. Lynn, S. L. Bud'ko, M. S. Torikachvili, N. Ni, S. Nandi, J. B. Leao, S. J. Poulton, D. N. Argyriou, B. N. Harmon, R. J. McQueeney, P. C. Canfield, and A. I. Goldman, Phys. Rev. B **78**, 184517 (2008).
[13] A. I. Goldman, A. Kreyssig, K. Prokes, D. K. Pratt, D. N. Argyriou, J. W. Lynn, S. Nandi, S. A. J. Kimber, Y. Chen, Y. B. Lee, G. Samolyuk, J. B. Leao, S. J. Poulton, S. L. Bud'ko, N. Ni, P. C. Canfield, B. N. Harmon, and R. J. McQueeney, Phys. Rev. B **79**, 024513 (2009).
[14] N. Kurita, M. Kimata, K. Kodama, A. Harada, M. Tomita, H. S. Suzuki, T. Matsumoto, K. Murata, S. Uji, and T. Terashima, Phys. Rev. B **83**, 100501(R) (2011).
[15] H. S. Jeevan, D. Kasinathan, H. Rosner, and P. Gegenwart, Phys. Rev. B **83**, 054511 (2011).
[16] P. C. Canfield and S. L. Bud'ko, Annu. Rev. Condens. Matter Phys. **1**, 27 (2010).
[17] E. Colombier, S. L. Bud'ko, N. Ni, and P. C. Canfield, Phys. Rev. B **79**, 224518 (2009).
[18] S. A. J. Kimber, A. Kreyssig, Y. Zhang, H. O. Jeschke, R. Valentí, F. Yokaichiya, E. Colombier, J. Yan, T. C. Hansen, T. Chatterji, R. J. McQueeney, P. C. Canfield, A. I. Goldman, and D. N. Argyriou, Nature Materials **4**, 471 (2009).
[19] D. C. Johnston, Adv. Phys. **59**, 803 (2010).
[20] C. Liu, G. D. Samolyuk, Y. Lee, Ni Ni, T. Kondo, A. F. Santander-Syro, S. L. Bud'ko, J. L. McChesney, E. Rotenberg, T. Valla, A. V. Fedorov, P. C. Canfield, B. N. Harmon, and A. Kaminski, Phys. Rev. Lett. **101**, 177005 (2008); C. Liu, T. Kondo, Ni Ni, A. D. Palczewski, A. Bostwick, G. D. Samolyuk, R. Khasanov, M. Shi, E. Rotenberg, S. L. Bud'ko, P. C. Canfield, and A. Kaminski, *ibid* **102**, 167004 (2009); C. Liu, T. Kondo, R. M. Fernandes, A. D. Palczewski, E. D. Mun, N. Ni, A. N. Thaler, A. Bostwick, E. Rotenberg, J. Schmalian, S. L. Bud'ko, P. C. Canfield, and A. Kaminski, Nature Physics **6**, 419 (2010).
[21] J. Fink, S. Thirupathaiah, R. Ovsyannikov, H. A. Dürr, R. Follath, Y. Huang, S. de Jong, M. S. Golden, Yu-Z. Zhang, H. O. Jeschke, R. Valent, C. Felser, S. D. Farahani, M. Rotter, and D. Johrendt, Phys. Rev. B **79**, 155118 (2009).
[22] M. F. Jensen, V. Brouet, E. Papalazarou, A. Nicolaou, A. Taleb-Ibrahimi, P. Le Fèvre, F. Bertran, A. Forget, and D. Colson, Phys. Rev. B **84**, 014509 (2011).
[23] Yogesh Singh, A. Ellern, and D. C. Johnston, Phys. Rev. B **79**, 094519 (2009); Yogesh Singh, M. A. Green, Q. Huang, A. Kreyssig, R. J. McQueeney, D. C. Johnston, and A. I. Goldman, Phys. Rev. B **80**, 100403R (2009); Yogesh Singh, M. A. Green, Q. Huang, A. Kreyssig, R. J. McQueeney, D. C. Johnston, and A. I. Goldman, Phys. Rev. B **80**, 100403R (2009); Abhishek Pandey, R. S. Dhaka, J. Lamsal, Y. Lee, V. K. Anand, A. Kreyssig, T. W. Heitmann, R. J. McQueeney, A. I. Goldman, B. N. Harmon, A. Kaminski and D. C. Johnston, Phys. Rev. Lett. **108**, 087005 (2012).
[24] W. H. Jiao, I. Felner, I. Nowik, and G.H. Cao, Journal of Superconductivity and Novel Magnetism **24**, 1287 (2011).
[25] S. Nandi, A. Kreyssig, Y. Lee, Y. Singh, J. W. Kim, D. C. Johnston, B. N. Harmon, and A. I. Goldman, Phys. Rev. B **79**, 100407(R) (2009).
[26] Y. Singh, Y. Lee, B. N. Harmon, and D. C. Johnston, Phys. Rev. B **79**, 220401(R) (2009).
[27] Y. Singh, Y. Lee, S. Nandi, A. Kreyssig, A. Ellern, S. Das, R. Nath, B. N. Harmon, A. I. Goldman, and D. C. Johnston, Phys. Rev. B **78**, 104512 (2008).
[28] R. Nath, Y. Singh, and D. C. Johnston, Phys. Rev. B **79**, 174513 (2009).
[29] B. Zhou, M. Xu, Y. Zhang, G. Xu, C. He, L. X. Yang, F. Chen, B. P. Xie, X.-Yu Cui, M. Arita, K. Shimada, H. Namatame, M. Taniguchi, X. Dai, and D. L. Feng, Phys. Rev. B **83**, 035110 (2011).
[30] B. Zhou, Y. Zhang, L. Yang, M. Xu, C. He, F. Chen, J. Zhao, H. Ou, J. Wei, B. Xie, T. Wu, G. Wu, M. Arita, K. Shimada, H. Namatame, M. Taniguchi, X. H. Chen, and D. L. Feng, Phys. Rev. B **81**, 155124 (2010).
[31] S. de Jong, E. van Heumen, S. Thirupathaiah, R. Huisman, F. Massee, J. B. Goedkoop, R. Ovsyannikov, J. Fink, H. A. Dürr, A. Gloskovskii, H. S. Jeevan, P. Gegenwart, A. Erb, L. Patthey, M. Shi, R. Follath, A. Varykhalov, and M. S. Golden, Europhysics Letters **89**, 27007 (2010).
[32] S. Thirupathaiah, E. D. L. Rienks, H. S. Jeevan, R.

Ovsyannikov, E. Slooten, J. Kaas, E. van Heumen, S. de Jong, H. A. Dürr, K. Siemensmeyer, R. Follath, P. Gegenwart, M. S. Golden, and J. Fink, Phys. Rev. B **84**, 014531 (2011).

[33] C. H. Lin, T. Berlijn, L. Wang, C. C. Lee, W. G. Yin, and W. Ku, Phys. Rev. Lett **107**, 257001 (2011).

[34] J. P. Perdew and Y. Wang, Phys. Rev. B **45**, 13244 (1992).

[35] S. Hufner, *Photoelectron Spectroscopy*, (Springer, Berlin, 1995), pp. 268–270.

[36] P. Starowicz, C. Liu, R. Khasanov, T. Kondo, G. Samolyuk, D. Gardenghi, Y. Lee, T. Ohta, B. Harmon, P. Canfield, S. Bud'ko, E. Rotenberg, and A. Kaminski, Phys. Rev. B **77**, 134520 (2008).

[37] T. Kondo, R. M. Fernandes, R. Khasanov, C. Liu, A. D. Palczewski, N. Ni, M. Shi, A. Bostwick, E. Rotenberg, J. Schmalian, S. L. Bud'ko, P. C. Canfield, and A. Kaminski, Phys. Rev. B **81**, 060507(R) (2010).

[38] A. Damasceli, Z. Hussain, and Z.-X. Shen, Rev. Mod. Phys. **75**, 473 (2003).

[39] C. Liu, A. D. Palczewski, R. S. Dhaka, T. Kondo, R. M. Fernandes, E. D. Mun, H. Hodovanets, A. N. Thaler, J. Schmalian, S. L. Bud'ko, P. C. Canfield, and A. Kaminski, Phys. Rev. B **84**, 020509(R) (2011).

[40] M. Yi, D. H. Lu, J. G. Analytis, J.-H. Chu, S.-K. Mo, R.-H. He, R. G. Moore, X. J. Zhou, G. F. Chen, J. L. Luo, N. L. Wang, Z. Hussain, D. J. Singh, I. R. Fisher, and Z.-X. Shen, Phys. Rev. B **80**, 024515 (2009).

[41] K. Terashima, Y. Sekiba, J. H. Bowen, K. Nakayama, T. Kawahara, T. Sato, P. Richard, Y.- M. Xu, L. J. Li, G. H. Cao, Z.-A. Xu, H. Ding, and T. Takahashi, Proceedings of the National Academy of Sciences **106**, 7330 (2009).

[42] G. Liu, H. Liu, L. Zhao, W. Zhang, X. Jia, J. Meng, X. Dong, J. Zhang, G. F. Chen, G. Wang, Y. Zhou, Y. Zhu, X. Wang, Z. Xu, C. Chen, and X. J. Zhou, Phys. Rev. B **80**, 134518 (2009).

[43] L. X. Yang, Y. Zhang, H. W. Ou, J. F. Zhao, D. W. Shen, B. Zhou, J. Wei, F. Chen, M. Xu, C. He, Y. Chen, Z. D. Wang, X. F. Wang, T. Wu, G. Wu, X. H. Chen, M. Arita, K. Shimada, M. Taniguchi, Z. Y. Lu, T. Xiang, and D. L. Feng, Phys. Rev. Lett. **102**, 107002 (2009).